Effects of van Hove singularities on magnetism and superconductivity in the t-t' Hubbard model: A parquet approach

V. Yu. Irkhin, A. A. Katanin, and M. I. Katsnelson
Institute of Metal Physics, 620219 Ekaterinburg, Russia
(Received 1 March 2001; published 3 October 2001)

The t-t' Hubbard model for the Fermi level near the van Hove singularity is considered within the renormalization group and parquet approaches. Interplay of ferromagnetic, antiferromagnetic, and superconducting channels is investigated, and the phase diagram of the model is constructed. In comparison with previous approaches, the account of ferromagnetic fluctuations suppresses superconducting pairing and, vice versa, the influence of the Cooper channel decreases the Curie temperature, so that the Stoner criterion is inapplicable even qualitatively.

DOI: 10.1103/PhysRevB.64.165107 PACS number(s): 75.10.−b, 74.20.−z, 71.10.−w

I. INTRODUCTION

Magnetic mechanisms of high-temperature superconductivity (HTSC) have become the subject of intensive investigations during last decades (see, e.g., Refs. 1–8). It was argued that the superconducting properties of HTSC materials are intimately related to their magnetic properties in the normal phase. In particular, many features of HTSC compounds were explained from the point of view of the competition of antiferromagnetic and superconducting order parameters.[6–8] A similar physical situation takes place in ruthenates like Sr_2RuO_4, where the interplay of ferromagnetism and p-wave superconductivity is of crucial importance.[9] Both copper-oxide systems and Sr_2RuO_4 are layered compounds. Therefore a general problem can be formulated as the investigation of the competition between magnetic and superconducting instabilities in two-dimensional (2D) electron systems.

On the other hand, the problem should be concretized. There are some evidences from both electron-structure calculations and experimental data that the Fermi surface (FS) of HTSC compounds at optimal doping or optimal pressure is close to the van Hove (VH) singularities of electron spectrum (see, e.g., Refs. 10–13); the situation in the ruthenates is similar.[14] Due to the presence of VH singularities, at VH band filling the density of states at the Fermi level becomes logarithmically divergent, which makes the Fermi liquid unstable with respect to magnetic ordering or superconductivity. One may expect *a priori* that near VH band fillings the physics is determined by VH points and is not sensitive to the form of the whole FS. This should be correct provided that FS is not nested, since in the nesting situation[15,16] the contribution of flat FS parts is also important.[17,18] As it was first discussed by Dzyaloshinskii,[19] the situation in 2D fermion system near VH fillings is similar in some respects to that in one-dimensional (1D) systems[20,21] or in 2D systems under the nesting condition.[22] It turned out that in the instability region the "normal" state can demonstrate a non-Fermi liquid behavior.[23]

The simplest model that gives a possibility to investigate the effects of VH singularities on magnetic ordering and superconductivity is the t-t' Hubbard model that takes into account nearest-neighbor and next-nearest-neighbor hopping. It is often discussed also in connection with HTSC compounds where the value $t'/t=-0.15$ was determined for La_2CuO_4 and the value $t'/t=-0.30$ for the Bi2212 system[24] (we neglect third-neighbor hopping t'' that does not lead to any qualitative changes).

The interplay of antiferromagnetism and superconductivity near VH fillings within the Hubbard model with $t'=0$ was first investigated in Refs. 19 and 25. It was shown that the leading instability in this case is antiferromagnetic one, and the transition temperature is close to its mean-field value. At the same time, the authors of Refs. 19 and 25 did not include the contribution of the particle-hole scattering at small momenta, as well as particle-particle scattering at momenta near $\mathbf{Q}=(\pi,\pi)$ by the reason that these contributions are logarithmic rather than double logarithmic. As we will argue in the present paper, even for weak-to-intermediate coupling regime these contributions should be also taken into account, which leads to an essential change of the results.

Recently, the authors of Ref. 26 have performed the renormalization group (RG) analysis of the states close to FS (not only near VH singularities) within an approach that is similar to that of Ref. 27. At $t'/t=-0.30$ they found competing antiferromagnetism and superconductivity, depending on the band filling. However, the approach of Ref. 27 also does not enable one to treat particle-hole scattering at small momenta on the equal footing with other contributions. As it was shown by the RG analysis in Ref. 28, the account of particle-hole scattering leads to occurrence of ferromagnetic phase at large enough $|t'|/t$; the criterion $t'/t<-0.27$ for the stability of ferromagnetism was obtained. At $-0.27<t'/t<0$ it was also found that either antiferromagnetism or superconductivity takes place. However, unlike Refs. 19, 25 and 26, the contributions of the Cooper channel were not taken into account in Ref. 28. The backward influence of the Cooper channel on magnetic ordering was investigated within the T-matrix approach.[29] It was found for the nondegenerate Hubbard model that the Cooper channel strongly suppresses the tendency to ferromagnetism, so that it is possible only for $t'/t<-0.35$. Numerical calculations[30] predict much larger values $(t'/t)_c$ for the stability of ferromagnetism at VH filling: $(t'/t)_c \gtrsim -0.47$.

 ©2001 The American Physical Society

Summarizing all these approaches, one can see that we need to consider on equal footing all four types of scattering to obtain the correct phase diagram, i.e., the particle-particle and particle-hole channels at both small momenta q and $\mathbf{q}\approx\mathbf{Q}$. The first step in this direction was made in Refs. 31 and 32 within the so-called two-patch approach. The authors of Refs. 31 and 32 wrote down approximate equations, which were very similar to the parquet equations in one dimension,[33] and obtained reasonable physical results. However, they also neglected particle-hole scattering at small momenta and particle-particle scattering at $\mathbf{q}\approx\mathbf{Q}$ at final stage.

Besides that, these 1D-like equations do not reproduce correctly all the peculiarities of the 2D dispersion law even close to VH singularities. From this point of view, most straightforward is the parquet approach of Refs. 19–22 (for a review see also Ref. 34). It was applied to the VH singularity problem in Refs. 19 and 25, but only the case $t'/t=0$ was considered (strictly speaking, this case requires an account of the whole FS because of nesting[17]).

In the present paper we consider different phases of the t-t' Hubbard model ($t'/t<0$) and construct the phase diagram near VH fillings within the approach.[20] Note that this approach is somewhat different from that used in later papers[22,19] and, as we will argue in this work, is more correct.

The outline of the paper is the following. In Sec. II we discuss noninteracting susceptibilities and consider the random-phase approximation (RPA). In Sec. III we consider two-patch equations with all four channels of scattering included and discuss the results of numerical solution of these equations. In Sec. IV we consider a full parquet approach to VH problem and compare the results with those of two-patch approach. In conclusion we summarize main results of the paper and discuss possible directions of further investigations.

II. THE MODEL AND RPA RESULTS

We consider t-t' Hubbard model on the square lattice:

$$H=\sum_{\mathbf{k}} \varepsilon_{\mathbf{k}} c^{\dagger}_{\mathbf{k}\sigma} c_{\mathbf{k}\sigma}+U\sum_{i} n_{i\uparrow}n_{i\downarrow} \tag{1}$$

with

$$\varepsilon_{\mathbf{k}}=-2t(\cos k_x+\cos k_y)+4t'\cos k_x\cos k_y+4t'-\mu, \tag{2}$$

where μ is the chemical potential (we have picked out $4t'$ for further convenience). We have already absorbed the sign of t' into Eq. (2), i.e., (hereafter we assume the transfer integrals t,t' to be positive. ($0\leqslant t'/t<1/2$).

The spectrum (2) contains VH singularities connected with the points $A=(\pi,0)$, $B=(0,\pi)$. These singularities lie at the Fermi surface for the filling with $\mu=0$ and arbitrary values of t'. For $t'=0$ the FS is nested, but the nesting is removed for $t'/t>0$.

Being expanded near the VH singularity points, the spectrum (2) takes the form

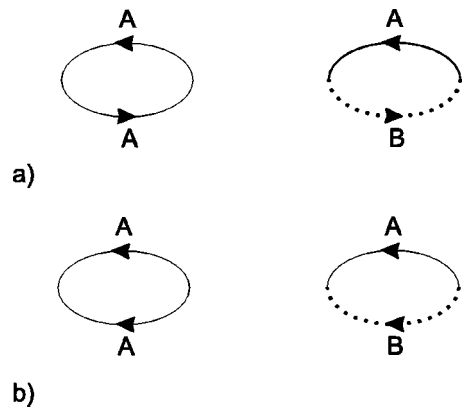

FIG. 1. Diagrams (bubbles) for noninteracting susceptibilities near $q=0$ and $\mathbf{q}=\mathbf{Q}$ in (a) Peierls channel (b) Cooper channel. Solid and dashed lines correspond to the electron Green functions near A and B singularities with the spectra (3a) and (3b), respectively.

$$\varepsilon^{A}_{\mathbf{k}}=-2t(\sin^2\varphi\overline{k_x}^2-\cos^2\varphi k_y^2)=-2tk_+k_--\mu, \tag{3a}$$

$$\varepsilon^{B}_{\mathbf{k}}=2t(\cos^2\varphi k_x^2-\sin^2\varphi\overline{k_y}^2)=2t\tilde{k}_+\tilde{k}_--\mu, \tag{3b}$$

where $\overline{k_x}=\pi-k_x$, $\overline{k_y}=\pi-k_y$,

$$\begin{aligned} k_{\pm}&=\sin\varphi\overline{k_x}\pm\cos\varphi k_y\\ \tilde{k}_{\pm}&=\cos\varphi k_x\pm\sin\varphi\overline{k_y}, \end{aligned} \tag{4}$$

φ is the half of the angle between asymptotes at VH singularity, $2\varphi=\cos^{-1}(2t'/t)$.

At $U=0$ we have the following results for the susceptibilities at small q and $\mathbf{q}\approx\mathbf{Q}=(\pi,\pi)$ [see Fig. 1(a)]:

$$\chi^{A}_{\mathbf{q}}=\sum_{\mathbf{k}}\frac{f(\varepsilon^{A}_{\mathbf{k}})-f(\varepsilon^{A}_{\mathbf{k}+\mathbf{q}})}{\varepsilon^{A}_{\mathbf{k}}-\varepsilon^{A}_{\mathbf{k}+\mathbf{q}}}=\frac{z_0}{4\pi^2t}(\xi_++\xi_-), \tag{5a}$$

$$\begin{aligned}\chi^{AB}_{\mathbf{q}+\mathbf{Q}}&=\sum_{\mathbf{k}}\frac{f(\varepsilon^{A}_{\mathbf{k}})-f(\varepsilon^{B}_{\mathbf{k}+\mathbf{q}})}{\varepsilon^{A}_{\mathbf{k}}-\varepsilon^{B}_{\mathbf{k}+\mathbf{q}}}\\ &=\frac{1}{2\pi^2t}\min(z_{\mathbf{Q}}\xi_+,z_{\mathbf{Q}}\xi_-,\xi_+\xi_-).\end{aligned} \tag{5b}$$

Here $f(\varepsilon)$ is the Fermi distribution function, $\xi_{\pm}=\min[\ln(\Lambda/q_{\pm}),\ln(\Lambda t^{1/2}/|\mu|^{1/2})]$, $q_{\pm}$ are defined in the same way as in Eq. (4),

$$z_0=1/\sqrt{1-R^2};\quad z_{\mathbf{Q}}=\ln[(1+\sqrt{1-R^2})/R], \tag{6}$$

and $R=2t'/t$. The expressions for $B\leftrightarrow A$ are obtained by replacing $\xi_+\rightarrow\tilde{\xi}_+$, $\xi_-\rightarrow-\tilde{\xi}_-$ where $\tilde{\xi}_{\pm}=\min[\ln(\Lambda/\tilde{q}_{\pm}),\ln(\Lambda t^{1/2}/|\mu|^{1/2})]$. The momentum dependence of $\chi_{\mathbf{q}}$ calculated with the spectra (2) is shown in Fig. 2(a). Since both the susceptibilities are divergent, we have at least two competing order parameters. In fact, two other polarization bubbles of Fig. 1(b), which are responsible for zero momentum and π pairing, are also divergent at small $\mathbf{q}$: [see also Fig. 2(b)]:

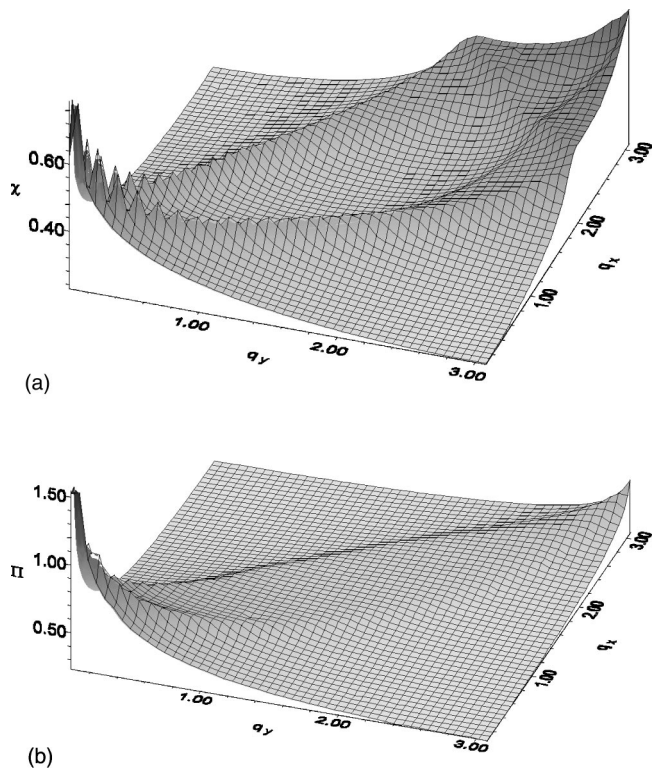

FIG. 2. The momentum dependence for (a) noninteracting susceptibility and (b) noninteracting Cooper response at $t'/t=0.3$.

$$\Pi^A_{\mathbf{q}}=\sum_{\mathbf{k}}\frac{1-f(\varepsilon^A_{\mathbf{k}})-f(\varepsilon^A_{\mathbf{k+q}})}{\varepsilon^A_{\mathbf{k}}+\varepsilon^A_{\mathbf{k+q}}}=\frac{c_0}{4\pi^2 t}\xi_+\xi_- \tag{7a}$$

$$\Pi^{AB}_{\mathbf{q+Q}}=\sum_{\mathbf{k}}\frac{1-f(\varepsilon^A_{\mathbf{k}})-f(\varepsilon^B_{\mathbf{k+q}})}{\varepsilon^A_{\mathbf{k}}+\varepsilon^B_{\mathbf{k+q}}}=\frac{c_{\mathbf{Q}}}{2\pi^2 t}\min(\xi_+,\xi_-), \tag{7b}$$

where

$$c_0=1/\sqrt{1-R^2};\quad c_{\mathbf{Q}}=\tan^{-1}(R/\sqrt{1-R^2})/R.$$

For $\Pi^B_{\mathbf{q}}$ we again have the replacements $A\to B$ and $\xi_+\to\tilde{\xi}_+$, $\xi_-\to-\tilde{\xi}_-$ in Eq. (7a).

In the RPA the expressions for particle-hole and particle-particle susceptibilities read

$$\overline{\chi}_{\mathbf{q}}=\frac{\chi_{\mathbf{q}}}{1-U\chi_{\mathbf{q}}} \tag{8}$$

$$\overline{\Pi}_{\mathbf{q}}=\frac{\Pi_{\mathbf{q}}}{1+U\Pi_{\mathbf{q}}}. \tag{9}$$

Thus Π decreases when the Coulomb interaction is taken into account, while χ increases and can diverge at some U. In particular, we have the conventional Stoner criterium of ferromagnetism $U\chi_0=1$, or

$$\frac{Uz_0}{2\pi^2 t}\ln\frac{\Lambda}{\rho}=1, \tag{10}$$

where $\rho^2=\max(T/t,|\mu|/t,\Delta/t)$ ($\Delta\sim\overline{S}$ is the spin splitting). The solution to this equation reads

$$\rho=\Lambda\exp[-2\pi^2\sqrt{t^2-(2t')^2}/U].$$

Therefore the ferromagnetism is present at any U; moreover, at $U\sim 2\pi^2[t^2-(2t')^2]^{1/2}$ one can expect that it becomes saturated. Similarly, considering the antiferromagnetic instability we obtain

$$\frac{U}{2\pi^2 t}\min\left(\ln^2\frac{\Lambda}{\rho},z_{\mathbf{Q}}\ln\frac{\Lambda}{\rho}\right)=1, \tag{11}$$

which gives

$$\rho=\Lambda\begin{cases}\exp(-\sqrt{2\pi^2 t/U}), & U/(2\pi^2 t)>1/z^2_{\mathbf{Q}}\\ \exp(-2\pi^2 t/z_{\mathbf{Q}}U), & U/(2\pi^2 t)<1/z^2_{\mathbf{Q}}\end{cases}$$

so that antiferromagnetism is favorable at small t'/t.

However, as it was discussed first by Dzyaloshinskii and coworkers, [19–22] RPA is incorrect even in the weak-coupling limit, except for the case when only one bubble is divergent. Since in the VH case all four bubbles of Fig. 1 are divergent, we have to use the parquet approach[19–22] instead of RPA. While in 1D case the parquet equations reduce to conventional differential RG equations (see, e.g., Refs. 17, 21 and 33), for higher space dimensionalities we have coupled integral equations. First we consider the application of the two-patch approach of Refs. 31 and 32 that uses mapping of the full parquet equations on an "effective" 1D problem.

III. TWO-PATCH EQUATIONS

The authors of Refs. 31 and 32 proposed the approach that neglects the difference between ξ_+ and ξ_- (and consequently between $\tilde{\xi}_+$ and $\tilde{\xi}_-$) and introduced a single-scaling variable $\xi=\min(\xi_+,\xi_-,\tilde{\xi}_+,\tilde{\xi}_-)$. Note that this approach is not strict, in particular because of the presence of double-logarithmic terms in Eqs. (5b) and (7a). At the same time, as we will see below (see also Ref. 32), this reproduces correctly main features of the exact parquet equations.

The two-patch equations read[31,32]

$$\begin{aligned}\gamma_1'&=2d_1(\xi)\gamma_1(\gamma_2-\gamma_1)+2d_2\gamma_1\gamma_4-2d_3\gamma_1\gamma_2\\ \gamma_2'&=d_1(\xi)(\gamma_2^2+\gamma_3^2)+2d_2(\gamma_1-\gamma_2)\gamma_4-d_3(\gamma_1^2+\gamma_2^2)\\ \gamma_3'&=-2d_0(\xi)\gamma_3\gamma_4+2d_1(\xi)\gamma_3(2\gamma_2-\gamma_1)\\ \gamma_4'&=-d_0(\xi)(\gamma_3^2+\gamma_4^2)+d_2(\gamma_1^2+2\gamma_1\gamma_2-2\gamma_2^2+\gamma_4^2),\end{aligned} \tag{12}$$

where $\gamma_i'\equiv d\gamma_i/d\xi$,

$$d_0(\xi)=2c_0\xi;\quad d_1(\xi)=2\min(\xi,z_Q)$$

$$d_2=2z_0;\quad d_3=2c_{\mathbf{Q}} \tag{13}$$

and four vertices γ_{1-4} are defined in Fig. 3. In these notations, $\gamma_i(0)=g_0\equiv U/(4\pi^2 t)$ corresponds to the Hubbard model. While only the case $d_2,d_3\ll d_0,d_1$ was considered in

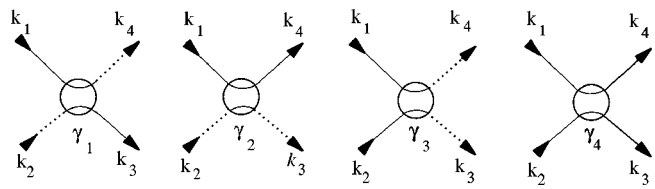

FIG. 3. The vertices $\gamma_i (i=1\ldots4)$. The solid lines inside the circles show which incoming and outgoing particles have the same spin projection.

Refs. 31 and 32, we perform a more general consideration where all the bubbles are taken into account. We have also taken into account the coefficient c_0 to treat correctly the t' dependence of the amplitude of particle-particle scattering. Note that the equations (12) are very similar to those in the 1D case[17,21,33] with the difference that in the latter case one has

$$d_0=d_2=0; \quad d_1=d_3=1. \tag{14}$$

The complete discussion of the physics of the equations (12) in the 1D case is given in Ref. 21. In two dimensions, the coefficients d_0 and d_1 become ξ dependent because of the presence of double-logarithmic terms. As we have already mentioned, this gives only approximate treatment of such terms. The equations (12) give a possibility to investigate the interplay of all the four scattering channels.

For ferromagnetic, antiferromagnetic, and d-wave superconducting susceptibilities we obtain (see Ref. 33)

$$\chi_{\mathrm{F,AF},d\text{-SC}}(\xi)=\int_0^{\xi} d\zeta d_{2,1,0}(\zeta)\mathcal{T}^2_{\mathrm{F,AF},d\text{-SC}}(\zeta), \tag{15}$$

where $\mathcal{T}$ satisfies the equation

$$\frac{d\ln\mathcal{T}_{\mathrm{F,AF},d\text{-SC}}}{d\xi}=\left\{\begin{array}{c} d_2(\gamma_1+\gamma_4) \\ d_1(\xi)(\gamma_2+\gamma_3) \\ d_0(\xi)(\gamma_3-\gamma_4)\end{array}\right\}. \tag{16}$$

The squared vertex in Eq. (15) has the same origin as in the RG equations (12). It arises after the application of Sudakov's trick[35] (see also the Appendix), which replaces $g_0\mathcal{T}(k_1\ldots k_4)$ by $\mathcal{T}^2(\zeta)$. The same result can be obtained directly by RG approach. Provided that γ_1 and γ_4 are simultaneously relevant, we have ferromagnetic ordering, while γ_2 and γ_3 lead to antiferromagnetic ordering. For the superconductivity, we have a more complicated combination of relevant and irrelevant vertices.

The results of the solution of equations (12)–(16) for various values of g_0 and t'/t are shown in Fig. 4. Depending on the values of g_0 and t'/t, ferromagnetic or antiferromagnetic susceptibility, or d-wave superconducting response diverges first. The parameter dependences of the critical energy scale $\mu_c=t\exp(-2\xi_c)$ are shown in Fig. 5. This scale can be approximately identified with the critical chemical potential or transition temperature. For comparison, the RPA results for the stability of ferromagnetic and antiferromagnetism are shown too. One can see that the values of transition temperatures obtained from the two-patch equations are much lower than the corresponding RPA results.

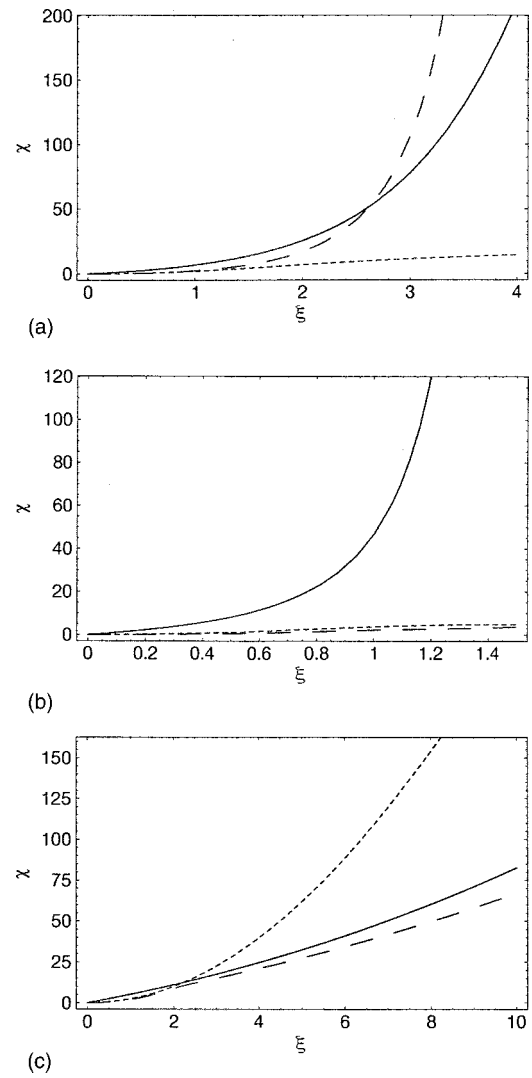

FIG. 4. The ferromagnetic (solid line), antiferromagnetic (long-dashed line), and d-wave superconducting (short-dashed line) susceptibilities for the two-patch model with (a) $t'/t=0.15$, $g_0=0.10$ (b) $t'/t=0.45$, $g_0=0.10$, (c) $t'/t=0.30$, $g_0=0.01$.

To understand qualitatively the nature of the critical temperature lowering, we may neglect the interpatch scattering. In the ferromagnetic case we have only one nonzero vertex γ_4, and the equation for it has the form

$$\gamma_4'=-2(z_0-c_0\xi)\gamma_4^2, \tag{17}$$

so that

$$\gamma_4=\frac{g_0}{1+g_0(c_0\xi^2-2z_0\xi)}. \tag{18}$$

The modification of the Stoner criterion takes the form

$$g_0\left(2z_0\ln\frac{\Lambda t^{1/2}}{|\mu|^{1/2}}-c_0\ln^2\frac{\Lambda}{\mu}\right)=1. \tag{19}$$

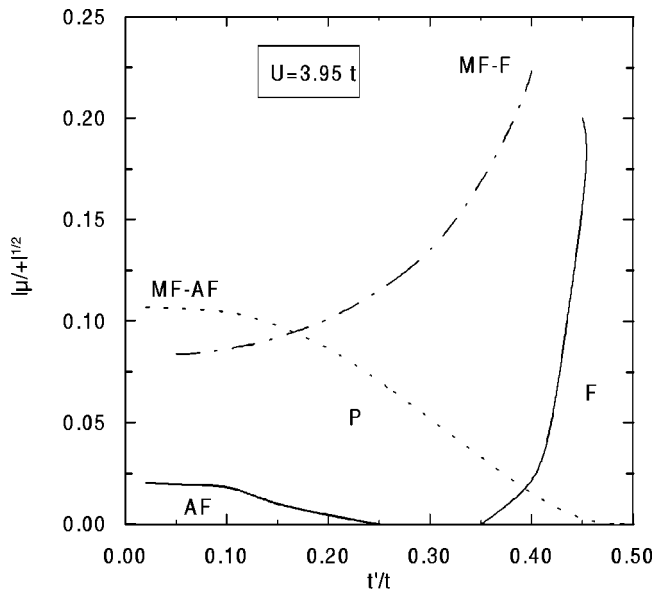

FIG. 5. The phase diagram for the two-patch model in μ-t'/t coordinates for $g_0=0.1$ $(U=3.95t)$. Dotted line is the mean-field boundary for antiferromagnetic phase, dot-dashed line for ferromagnetic one.

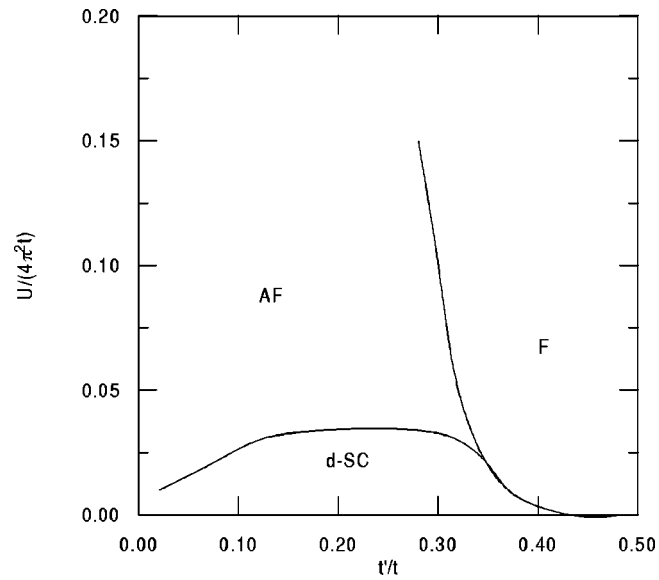

FIG. 6. The phase diagram for the two-patch model in g_0-t'/t coordinates at van Hove filling $(\mu=0)$.

Then we have from Eq. (19) at $z_0=c_0$ (which is the case of t-t' model)

$$\ln\frac{\Lambda t^{1/2}}{|\mu|^{1/2}}=1-\sqrt{1-\frac{1}{z_0g_0}}>\frac{1}{2z_0g_0}$$

(for R close to unity we have $z_0g_0>1$). Thus, the decrease of the Curie temperature in comparison with the mean-field approach $(c_0=0)$ is directly connected with the account of the Cooper bubble, which is in agreement with the T-matrix approximation.[29] Note, however, that the structure of Eq. (18) is different from that obtained in the T-matrix approach.

The resulting phase diagram in U-t'/t plane with all the scattering channels being included is shown in Fig. 6. One can see that the d-wave superconducting response is strongly suppressed by particle-hole scattering processes. This is the leading divergent response only at small values of coupling constant $g_0<0.04$, which corresponds to $U<1.6t$. The critical temperature in this region is also exponentially small $[T_c\sim\mu_c\sim\exp(-1/g_0)]$.

IV. PARQUET EQUATIONS

Now we pass to the consideration of the full parquet equations and compare the results of their solution with approximate RG equations of Sec. II. We use the generalization of the approach of Ref. 20 to the case of two dimensions.

In the parquet approach (see the Appendix) we have for each vertex $i=1\ldots4$ three types of bricks, which are shown in Fig. 7: the Cooper brick $C_i(\xi_\pm,\eta_\pm)$, and two zero-sound bricks, $Z_i(\xi_\pm,\eta_\pm)$ and $\tilde{Z}_i(\xi_\pm,\eta_\pm)$. Up to a logarithmic accuracy, they depend on $\xi_\pm=\ln(\Lambda/k_\pm)$ and $\eta_\pm=\ln(\Lambda/q_\pm)$ only, $k_\pm=k_{1\pm}+k_{2\pm}$ and $q_\pm=\max\{k_{3\pm}-k_{1\pm},k_{3\pm}-k_{2\pm}\}$ being the Cooper and zero-sound momenta transfer. Note that, because of the presence of double logarithms, we cannot restrict ourselves *a priori* to considering the case $\xi_+\sim\xi_-$ and $\eta_+\sim\eta_-$, but have to treat a more general case. The vertices $\gamma_i(\xi_\pm,\eta_\pm)$ in different regions of $\xi_\pm$ and $\eta_\pm$ are given by[20]

$$\gamma_i(\xi_\pm,\eta_\pm)=\gamma_i^h(\xi_\pm,\eta_\pm)\equiv g_0+C_i(\xi_\pm,\eta_\pm)+Z_i(\eta_\pm,\eta_\pm)+\tilde{Z}_i(\eta_\pm,\eta_\pm)(\xi_\pm>\eta_\pm),$$

$$\gamma_i(\xi_\pm,\eta_\pm)=\gamma_i^l(\xi_\pm,\eta_\pm)\equiv g_0+C_i(\xi_\pm,\xi_\pm)+Z_i(\xi_\pm,\eta_\pm)+\tilde{Z}_i(\xi_\pm,\xi_\pm)(\xi_\pm<\eta_\pm,\eta_\pm^{(1)}<\eta_\pm^{(2)}),$$

$$\gamma_i(\xi_\pm,\eta_\pm)=\tilde{\gamma}_i^l(\xi_\pm,\eta_\pm)\equiv g_0+C_i(\xi_\pm,\xi_\pm)+Z_i(\xi_\pm,\xi_\pm)+\tilde{Z}_i(\xi_\pm,\eta_\pm)(\xi_\pm<\eta_\pm,\eta_\pm^{(1)}>\eta_\pm^{(2)}),\qquad(20)$$

where $\eta_\pm^{(1,2)}=\ln(\Lambda/|k_{3\pm}-k_{1,2\pm}|)$. Following Ref. 20, we have taken into account that at $\xi_\pm>\eta_\pm$ the Cooper brick depends on both $\xi_\pm$ and $\eta_\pm$, while the zero-sound bricks depend only on $\eta_\pm$. Vice versa, at $\xi_\pm<\eta_\pm$ the Cooper brick and one of the zero-sound bricks depend only on $\xi_\pm$, and another zero-sound brick depends on both $\xi_\pm$ and $\eta_\pm$.

When all momenta are of the same order of magnitude, i.e. $\xi_\pm=\eta_\pm$, the vertices

$$\gamma_i(\xi_\pm,\xi_\pm)=\gamma_i(\xi_\pm)\qquad(21)$$

are analogous to those introduced in Sec. III with the only difference that now they depend on two scaling variables $\xi_\pm$. However, unlike the 1D case, the parquet equations do not reduce to the equations for $\gamma_i(\xi_\pm)$, but contain the full dependence $\gamma_i(\xi_\pm,\eta_\pm)$. The corresponding equations are presented in the Appendix. As discussed in Appendix, the

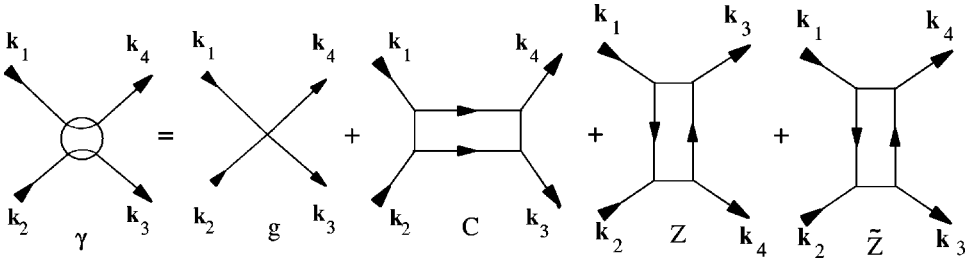

FIG. 7. The representation of the vertex in the parquet approach as a sum of bricks for the Cooper (C) and zero-sound ($Z,\tilde{Z}$) channels.

approach we use gives a possibility to treat the 2D situation in a more correct way in comparison with the approach of Refs. 22 and 19.

The parquet equations were solved numerically. To this end, we placed the variables ξ,η on a grid with 16 points in each dimension, so that the total number of vertices to be taken into account is $3\times4\times16^4\approx8\times10^6$. It is important that the grid was chosen for the logarithmic variables ξ,η, but not for the momenta themselves. This gives a possibility to use simple integration methods (e.g., the trapezium method) to obtain the results that are correct to logarithmic accuracy. The resulting system of 8×10^6 algebraic equations was solved by the Zeidel method.

The structure of the solutions of the parquet equations is quite similar to that in the two-patch approach, except for that now we have momenta-dependent vertices. Again, the relevance of γ_1 and γ_4 with $\xi_\pm=\eta_\pm=\xi$ leads to ferromagnetic ordering, while the relevance of γ_2 and γ_3 at $\xi_\pm=\eta_\pm=\xi$ to antiferromagnetic one. The results of solution of the parquet equations are shown in Figs. 8 and 9. One can see that the results coincide qualitatively with those of the two-patch parquet approach of Sec. III. At not too large t'/t, the antiferromagnetic instability occurs first, while for t'/t close to 1/2 the leading instability is ferromagnetic one. The superconductivity occurs also only for very small g_0.

The transition temperatures obtained within the parquet approach are larger than those obtained from two-patch equations, but are still lower than the RPA results. In particular, in the limit of small t'/t the parquet calculations,[19,25] which do not take into account single-logarithmic contributions of the loops Figs. 1(a), and 1(d), yield for $g_0=0.1$ the critical value for stability of antiferromagnetism $\xi_c^2=5.2$, which is close to RPA result, $\xi_c^2=5.0$. At the same time, our parquet calculations give larger value, $\xi_c^2=6.37$ (the result of two-patch equations is $\xi_c^2=18.2$). The region of stability of d-wave superconducting phase is even smaller than that obtained from two-patch equations.

The critical concentrations n_c for the stability of ferromagnetic, antiferromagnetic or superconducting phases close to VH filling can be estimated from the critical chemical potential with the use of the condition

$$n=\sum_{\mathbf{k}} f(\varepsilon_{\mathbf{k}}). \tag{22}$$

Using the form of spectrum (2) and taking the limit of filling close to VH one, we obtain for $|\mu|\ll t$

$$\delta n_c=n_c-n_{\mathrm{VH}}=\frac{\mu_c}{2\pi^2 t\sqrt{1-R^2}}\ln\frac{\Lambda t^{1/2}}{\mu_c^{1/2}}\simeq\frac{\xi_c\exp(-2\xi_c)}{2\pi^2\sqrt{1-R^2}}, \tag{23}$$

where n_{VH} is the VH filling. In particular, for $g_0=0.1$ ($U=3.95t$) we have from Fig. 8

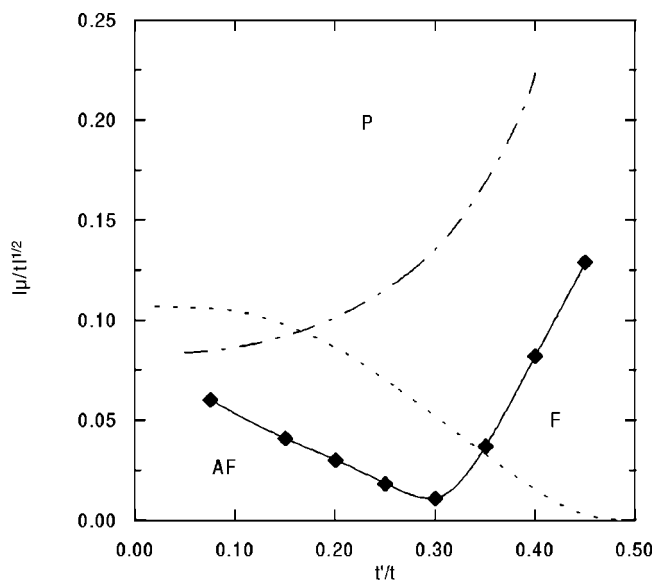

FIG. 8. The phase diagram from parquet equations in μ-t'/t coordinates for $g_0=0.1$ ($U=3.95t$). The lines are the same as in Fig. 5.

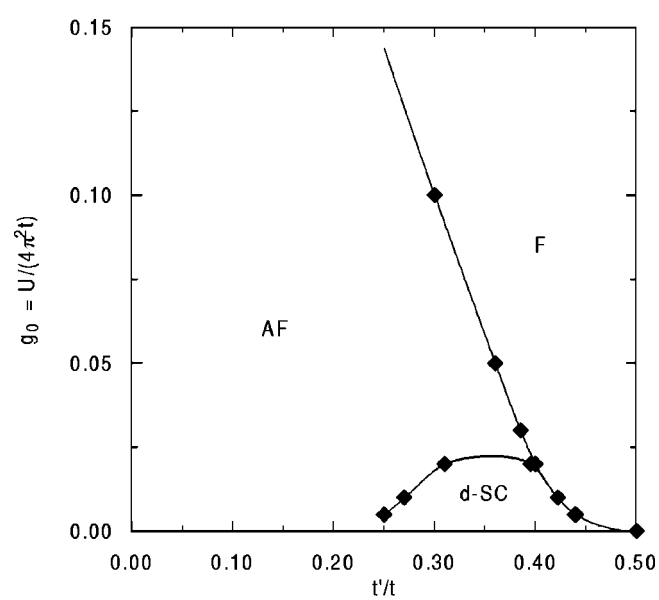

FIG. 9. The phase diagram from parquet equations for van Hove filling ($\mu=0$) in g_0-t'/t coordinates.

$$\delta n_c = 0.01 \quad (\text{AF phase}, \quad t'/t \to 0),$$

$$\delta n_c = 0.03 \quad (\text{F phase}, \quad t'/t = 0.45). \tag{24}$$

Thus, except for the limit $R \to 1$ $(t' \to t/2)$, the critical concentrations are very small, which is in qualitative agreement with the results of Ref. 29. Because of the exponential smallness of the critical chemical potential, the critical concentrations for the superconducting phase are even smaller than those for the magnetically ordered phases.

V. CONCLUSION

Now we summarize the main results of the paper. Using the two-patch equations (Sec. III) and parquet equations (Sec. IV) we constructed the phase diagrams of t-t' Hubbard model (Figs. 5, 6, 8, and 9) at the fillings that are close to the van Hove one. It was argued that the simultaneous account of all the scattering channels is important in considering the VH problem, the smallness of contributions of some channels (logarithmical vs double-logarithmical divergence) being compensated by the growth of relevant couplings. Both the approaches used, two-patch and parquet ones, give similar phase diagrams. In agreement with the previous approaches,[28–30] antiferromagnetism is favorable for small t'/t, while ferromagnetism for larger values of t'/t. The stability of antiferromagnetism and especially ferromagnetism is greatly reduced in comparison with the corresponding mean-field criteria. Thus the Stoner criterion is completely inapplicable for the systems with VH singularities; depending on the value t'/t, it overestimates the critical temperature by two to ten times. This conclusion is in qualitative agreement with the results of Ref. 29. Besides that, the mean-field approach is unable to determine the critical value $(t'/t)_c$ which separates the ferromagnetic and antiferromagnetic phases.

Unlike Ref. 28, $(t'/t)_c$ turns out to be U dependent and decreases with increasing U. Although the RG (and also parquet) approach is unable to describe the ordered states, from scaling arguments we have $\overline{S} \propto (\mu_c/t)^{\beta}$, where β is the magnetization critical exponent. With increasing U, the ferromagnetic and antiferromagnetic states are characterized by large magnetic moments, and ferromagnetism possibly becomes saturated. However, these values of U are not described by perturbative approaches and should be treated in the strong-coupling limit. At the same time, determining parameters of the ferro-antiferromagnetic quantum-phase transition would be of interest, especially the critical exponents. One can expect that they are independent of the coupling.

Another result of the paper is that the tendency to d-wave superconducting pairing is considerably reduced in comparison with the treatments of Refs. 28 and 26: it can occur only at very small values of U. Of course, this concerns only the pairing due to the VH singularities themselves; the pairing can be further enhanced by other factors. This can be also the subject for future investigations. Details of the electron spectrum, especially the form of the fermion Green's functions close to the phase transition into the ferromagnetic or antiferromagnetic state are beyond the scope of the present paper. Although the marginal[36] and non-Fermi-liquid behavior[23] was found (see also the discussion in Ref. 37), this problem needs further investigations, since a simultaneous account of all the scattering channels can be important in this case too. For example, only one of four scattering channels was included in Ref. 23.

We believe that the results of the present paper can be also important for the theory of itinerant-electron ferromagnetism. A standard consideration (including contemporary spin-fluctuation theories[38]) starts from the RPA approach. It was noted in Ref. 39 that for almost all known itinerant-electron ferromagnets the Fermi level lies near a 2D-like VH singularity. This is a result of merging two weaker 3D square-root singularities along symmetrical directions in the Brillouin zone.[40] We have shown that under such conditions the RPA approach and the Stoner criterion are not applicable even qualitatively because of the strong interference with the Cooper channel. Of course, the effect of the logarithmic VH singularity in the 3D case is not exactly the same as in the pure 2D case considered here, so that the 3D problem needs further investigations. However, the naive Stoner criterion is in any case doubtful and needs a careful justification.

In this respect, it would be interesting to generalize the results of the present paper (at least those from the two-patch equations) on the degenerate-band Hubbard model. As was argued in Ref. 29, in this case the suppression of ferromagnetic ordering is much weaker than for the nondegenerate model considered. One can also expect that the particle-hole scattering with small momenta will not renormalize superconducting channel as strongly as for the nondegenerate model. However, these statements need further justification since the diagram series in the degenerate and nondegenerate cases look like rather similar.

ACKNOWLEDGMENT

The research described was supported in part by Grant No. 00-15-96544 from the Russian Basic Research Foundation (Support of Scientific Schools).

APPENDIX: THE PARQUET APPROACH IN ONE AND TWO DIMENSIONS

First we consider the simple model of spinless fermions

$$H = \sum_{\mathbf{k}} \varepsilon_{\mathbf{k}} c^{\dagger}_{\mathbf{k}} c_{\mathbf{k}} + \sum_{\mathbf{k},\mathbf{p}} g(\mathbf{p}) c^{\dagger}_{\mathbf{k}} c_{\mathbf{k}-\mathbf{p}} c^{\dagger}_{\mathbf{k}} c_{\mathbf{k}+\mathbf{p}} \tag{A1}$$

with $g(k_F) = g_0$. In one dimension we have the representation[20] for the renormalized vertex γ (Fig. 5)

$$\gamma(\xi,\eta) = g_0 + C(\xi,\eta) + Z_1(\xi,\eta) + Z_2(\xi,\eta), \tag{A2}$$

where the bricks are given by

$$C(\xi,\eta) = -c \int_0^{\xi} d\zeta\, \gamma^c(\overline{\zeta,\eta})\, \gamma^h(\zeta,\eta), \quad \xi > \eta$$

$$Z_{1,2}(\xi,\eta)=z_{1,2}\int_0^{\eta}d\zeta\,\gamma_{1,2}^{z}(\overline{\zeta,\xi})\,\gamma_{1,2}^{l}(\zeta,\eta),\quad \xi<\eta, \tag{A3}$$

and $\xi=\ln(\Lambda/|k_1+k_2|)$; $\eta=\ln(\Lambda/\max\{k_3-k_1,k_3-k_2\})$. Here the definition is used

$$\overline{\zeta,\xi}=\begin{cases}\zeta & |\zeta|<|\xi|\\ \xi & |\zeta|>|\xi|\end{cases}, \tag{A4}$$

and we assume that the Cooper and zero-sound (Z and $\tilde{Z}$) loops are logarithmically divergent with the coefficients c and $z_{1,2}$, respectively (we generalize here the approach of Ref. 20 to the case where both the channels, Z and $\tilde{Z}$ contain divergences). The vertices in Eq. (A3) are given by

$$\begin{aligned}\gamma^{c}(\xi)&=g_0+Z_1(\xi,\xi)+Z_2(\xi,\xi),\\ \gamma_{1,2}^{z}(\xi)&=g_0+C(\xi,\xi)+Z_{2,1}(\xi,\xi),\\ \gamma^{h}(\xi,\eta)&=\gamma^{c}(\xi)+C(\xi,\eta),\\ \gamma_{1,2}^{l}(\xi,\eta)&=\gamma_{1,2}^{z}(\xi)+Z_{1,2}(\xi,\eta).\end{aligned} \tag{A5}$$

The equations (A2)–(A5) form the closed system of parquet equations for the 1D spinless case. The validity of these equations can be demonstrated for the simple case where only one bubble is divergent, e.g., $z_1=z_2=0$, so that the direct ladder (RPA) summation is possible. In this case $Z_{1,2}(\xi,\eta)=0$, $\gamma^{c}(\xi)=g_0$, and we obtain from (A2) and (A5) the standard ladder equation

$$\gamma(\xi,\eta)=g_0-cg_0\xi\gamma(\xi,\eta). \tag{A6}$$

This has the solution

$$\gamma(\xi,\eta)=\frac{g_0}{1+cg_0\xi}. \tag{A7}$$

Now we return to the general case $z_1,z_2,c\neq 0$. As it is shown in Ref. 20, the equations (A2)–(A5) at $\xi=\eta$ can be reduced to

$$\gamma(\xi,\xi)\equiv\gamma(\xi)=g_0+(z_1+z_2-c_0)\int_0^{\xi}\gamma^2(\zeta)d\zeta \tag{A8}$$

which is equivalent to the differential RG equation

$$\frac{d\gamma}{d\xi}=(z_1+z_2-c)\gamma^2. \tag{A9}$$

Since in one dimension $z_1=c$, $z_2=0$, γ is marginal and we have a Luttinger-liquid behavior.[27,33,17] Alternatively, the equation (A8) or (A9) can be obtained directly with the use of the Sudakov's trick[35] or standard RG approach[27] without considering the general dependence $\gamma(\xi,\eta)$. Thus, in the 1D case the parquet and RG approaches are equivalent.

In the 2D case we have two pairs of variables, $\xi_\pm$ and $\eta_\pm$. Moreover, unlike the 1D case, now two possibilities occur: the momentum integration in bubbles can be logarithmical or double logarithmical. For example, we consider the case where the integration in the Cooper bubble is double logarithmic while in the zero-sound channel this yields only simple logarithms (which is similar to the situation for VH singularities). Then it can be checked by a direct comparison with perturbation theory that the equations

$$C(\xi_\pm,\eta_\pm)=-cg_0\int_0^{\xi_+}\int_0^{\xi_-}d\zeta_+d\zeta_-\gamma^{c}(\overline{\zeta_\pm,\eta_\pm})\gamma^{h}(\zeta_\pm,\eta_\pm),\quad \xi_\pm>\eta_\pm$$

$$\begin{aligned}Z_{1,2}(\xi_\pm,\eta_\pm)&=z_{1,2}g_0\int_0^{\eta_+}d\zeta_+\gamma_{1,2}^{z}(\overline{\zeta_+,\xi_+},\xi_-)\gamma_{1,2}^{l}(\zeta_+,\eta_-;\eta_\pm)\\ &\quad+z_{1,2}g_0\int_0^{\eta_-}d\zeta_-\gamma_{1,2}^{z}(\xi_+,\overline{\zeta_-,\xi_-})\gamma_{1,2}^{l}(\eta_+,\zeta_-;\eta_\pm),\\ &\qquad\xi_\pm<\eta_\pm\end{aligned} \tag{A10}$$

with

$$\begin{aligned}\gamma^{c}(\eta_\pm)&=g_0+Z_1(\eta_\pm,\eta_\pm)+Z_2(\eta_\pm,\eta_\pm)\\ \gamma_i^{z}(\xi_\pm)&=g_0+C_i(\xi_\pm,\xi_\pm)+Z_{3-i}(\xi_\pm,\xi_\pm)\\ \gamma^{h}(\xi_\pm,\eta_\pm)&=\gamma^{c}(\eta_\pm)+C(\xi_\pm,\eta_\pm)\\ \gamma_i^{l}(\xi_\pm,\eta_\pm)&=\gamma_i^{z}(\xi_\pm)+Z_i(\xi_\pm,\eta_\pm)\end{aligned} \tag{A11}$$

give the parquet solution of the problem. Note that beyond one dimension the integral parquet equations do not reduce to differential ones.

The above approach is different from the approach of Refs. 22, 19, and 17 where a standard RG scheme was applied in one dimension, while momentum dependence in another dimension was taken into account exactly rather than to logarithmic accuracy. However, the applicability of last approach is doubtful. Indeed, in the 1D case the equation (A8) can be considered as a logarithmic approximation to the Bethe-Salpeter equations

$$\begin{aligned}C(k_1,k_2,k_3)&=g_0-c_0g_0\int_0^{\Lambda}dk\,\gamma(k_1+k,k_2-k,k_3)\\ Z_1(k_1,k_2,k_3)&=g_0+z_1g_0\int_0^{\Lambda}dk\,\gamma(k_1,k_3+k,k_3)\\ Z_2(k_1,k_2,k_3)&=g_0+z_2g_0\int_0^{\Lambda}dk\,\gamma(k_1,k_2+k,k_3+k).\end{aligned} \tag{A12}$$

In the 2D case where we have *both* slow and fast momenta we need to combine Eqs. (A8) and (A12) which is impossible since Eq. (A8) is quadratic in γ while Eq. (A12) is *linear*. The equations of Refs. 22, 19 and 17

$$C(k_1,k_2,k_3,\xi)=g_0-c_0\int_0^{\xi}d\zeta\int_0^{\Lambda}dk\,\gamma(k_1,k_2,k_3+k;\zeta)\times\gamma(k_1+k,k_2-k,k_3;\zeta)$$

$$Z_1(k_1,k_2,k_3,\xi)=g_0+z_1\int_0^{\xi}d\zeta\int_0^{\Lambda}dk\,\gamma(k_1,k_3+k,k_3;\zeta)\times\gamma(k_1+k,k_2,k_3+k;\zeta)$$

$$Z_2(k_1,k_2,k_3,\xi)=g_0+z_2\int_0^{\xi}d\zeta\int_0^{\Lambda}dk\,\gamma(k_1,k_2+k,k_3+k;\zeta)\,\gamma(k_3+k,k_2,k_3;\zeta) \tag{A13}$$

are not fully correct. If we suppose that γ does not depend on ξ, we do not reproduce the 1D Bethe-Salpeter equations (A12). At the same time, the approach of Ref. 20 is free from these problems.

The generalization of equations (A10) to the full VH problem is trivial. The parquet equations have the form

$$C_1(\xi_\pm,\eta_\pm)=-c_{\mathbf{Q}}\int_{c_{\mathbf{Q}}}[\gamma_1^c(\overline{\zeta_\pm,\eta_\pm})\gamma_2^h(\xi_\pm,\zeta_\pm)+\gamma_2^c(\overline{\zeta_\pm,\eta_\pm})\gamma_1^h(\xi_\pm;\zeta_\pm)],$$

$$\begin{aligned}Z_1(\xi_\pm;\eta_\pm)=z_{\mathbf{Q}}\int_{z_{\mathbf{Q}}}[&\gamma_1^z(\overline{\zeta_\pm,\xi_\pm})\tilde{\gamma}_2^l(\xi_\pm,\zeta_\pm)\\&+\tilde{\gamma}_2^z(\overline{\zeta_\pm,\xi_\pm})\gamma_1^l(\xi_\pm,\zeta_\pm)\\&-2\gamma_1^z(\overline{\zeta_\pm,\xi_\pm})\gamma_1^l(\xi_\pm,\zeta_\pm)\\&+\gamma_3^z(\overline{\zeta_\pm,\xi_\pm})\tilde{\gamma}_3^l(\xi_\pm,\zeta_\pm)\\&+\tilde{\gamma}_3^z(\overline{\zeta_\pm,\xi_\pm})\gamma_3^l(\xi_\pm,\zeta_\pm)\\&-2\gamma_3^z(\overline{\zeta_\pm,\xi_\pm})\gamma_3^l(\xi_\pm,\zeta_\pm)],\end{aligned}$$

$$\tilde{Z}_1(\xi_\pm;\eta_\pm)=z_0\int_{z_0}^{A}\tilde{\gamma}_4^z(\overline{\zeta_\pm,\xi_\pm})\tilde{\gamma}_1^l(\zeta_\pm,\eta_\pm)+z_0\int_{z_0}^{B}\gamma_1^z(\overline{\zeta_\pm,\xi_\pm})\tilde{\gamma}_4^l(\zeta_\pm,\eta_\pm);$$

$$C_2(\xi_\pm,\eta_\pm)=-c_{\mathbf{Q}}\int_{c_{\mathbf{Q}}}[\gamma_1^c(\overline{\zeta_\pm,\eta_\pm})\gamma_1^h(\xi_\pm,\zeta_\pm)+\gamma_2^c(\overline{\zeta_\pm,\eta_\pm})\gamma_2^h(\xi_\pm,\zeta_\pm)],$$

$$\begin{aligned}Z_2(\xi_\pm;\eta_\pm)=z_0\int_{z_0}^{A}[&\tilde{\gamma}_4^z(\overline{\zeta_\pm,\xi_\pm})\gamma_2^l(\zeta_\pm,\eta_\pm)\\&+\gamma_4^z(\overline{\zeta_\pm,\xi_\pm})\tilde{\gamma}_1^l(\zeta_\pm,\eta_\pm)\\&-2\gamma_4^z(\overline{\zeta_\pm,\xi_\pm})\gamma_2^l(\zeta_\pm,\eta_\pm)]\\&+z_0\int_{z_0}^{B}[\tilde{\gamma}_1^z(\overline{\zeta_\pm,\xi_\pm})\gamma_4^l(\zeta_\pm,\eta_\pm)\\&+\gamma_2^z(\overline{\zeta_\pm,\xi_\pm})\tilde{\gamma}_4^l(\zeta_\pm,\eta_\pm)\\&-2\gamma_2^z(\overline{\zeta_\pm,\xi_\pm})\gamma_4^l(\zeta_\pm,\eta_\pm)],\end{aligned}$$

$$\tilde{Z}_2(\xi_\pm;\eta_\pm)=z_{\mathbf{Q}}\int_{z_{\mathbf{Q}}}[\tilde{\gamma}_2^z(\overline{\zeta_\pm,\xi_\pm})\tilde{\gamma}_2^l(\zeta_\pm,\eta_\pm)+\tilde{\gamma}_3^z(\overline{\zeta_\pm,\xi_\pm})\tilde{\gamma}_3^l(\zeta_\pm,\eta_\pm)];$$

$$C_3(\xi_\pm;\eta_\pm)=-c_0\int_{c_0}^{A}\gamma_4^c(\overline{\zeta_\pm,\eta_\pm})\gamma_3^h(\xi_\pm,\zeta_\pm)-c_0\int_{c_0}^{B}\gamma_3^c(\overline{\zeta_\pm,\eta_\pm})\gamma_4^h(\xi_\pm,\zeta_\pm),$$

$$\begin{aligned}Z_3(\xi_\pm;\eta_\pm)=z_{\mathbf{Q}}\int_{z_{\mathbf{Q}}}[&\gamma_3^z(\overline{\zeta_\pm,\xi_\pm})(\tilde{\gamma}_2^l(\zeta_\pm,\eta_\pm)-\gamma_1^z(\zeta_\pm,\eta_\pm))\\&+(\tilde{\gamma}_2^z(\overline{\zeta_\pm,\xi_\pm})-\tilde{\gamma}_1^z(\overline{\zeta_\pm,\xi_\pm}))\gamma_3^l(\zeta_\pm,\eta_\pm)\\&+\gamma_1^z(\overline{\zeta_\pm,\xi_\pm})(\tilde{\gamma}_3^l(\zeta_\pm,\eta_\pm)-\gamma_3^l(\zeta_\pm,\eta_\pm))\\&+(\tilde{\gamma}_3^z(\overline{\zeta_\pm,\xi_\pm})-\gamma_3^z(\overline{\zeta_\pm,\xi_\pm}))\gamma_1^l(\zeta_\pm,\eta_\pm)],\end{aligned}$$

$$\tilde{Z}_3(\xi_\pm;\eta_\pm)=z_{\mathbf{Q}}\int_{z_{\mathbf{Q}}}[\tilde{\gamma}_3^z(\overline{\zeta_\pm,\xi_\pm})\tilde{\gamma}_2^l(\zeta_\pm,\eta_\pm)+\tilde{\gamma}_2^z(\overline{\zeta_\pm,\xi_\pm})\tilde{\gamma}_3^l(\zeta_\pm,\eta_\pm)];$$

$$C_4(\xi_\pm;\eta_\pm)=-c_0\int_{c_0}^{A}\gamma_3^c(\overline{\zeta_\pm,\eta_\pm})\gamma_3^h(\xi_\pm,\zeta_\pm)-c_0\int_{c_0}^{B}\gamma_4^c(\overline{\zeta_\pm,\eta_\pm})\gamma_4^h(\xi_\pm,\zeta_\pm),$$

$$\begin{aligned}Z_4(\xi_\pm;\eta_\pm)=z_0\int_{z_0}^{A}[&\gamma_4^z(\overline{\zeta_\pm,\xi_\pm})\tilde{\gamma}_4^l(\zeta_\pm,\eta_\pm)\\&+\tilde{\gamma}_4^z(\overline{\zeta_\pm,\xi_\pm})\gamma_4^l(\zeta_\pm,\eta_\pm)\\&-2\gamma_4^z(\overline{\zeta_\pm,\xi_\pm})\gamma_4^l(\zeta_\pm,\eta_\pm)]\\&+z_0\int_{z_0}^{B}[\gamma_2^z(\overline{\zeta_\pm,\xi_\pm})\tilde{\gamma}_1^l(\zeta_\pm,\eta_\pm)\\&+\tilde{\gamma}_1^z(\overline{\zeta_\pm,\xi_\pm})\gamma_2^l(\zeta_\pm,\eta_\pm)\\&-2\gamma_2^z(\overline{\zeta_\pm,\xi_\pm})\gamma_2^l(\zeta_\pm,\eta_\pm)],\end{aligned}$$

$$\tilde{Z}_4(\xi_\pm;\eta_\pm)=z_0\int_{z_0}^{A}\tilde{\gamma}_4^z(\overline{\zeta_\pm,\xi_\pm})\tilde{\gamma}_4^l(\zeta_\pm,\eta_\pm)+z_0\int_{z_0}^{B}\tilde{\gamma}_1^z(\overline{\zeta_\pm,\xi_\pm})\tilde{\gamma}_1^l(\zeta_\pm,\eta_\pm). \quad \text{(A14)}$$

The vertices are now given by

$$\begin{aligned}
\gamma_i^c(\eta_\pm)&=g_0+Z_i(\eta_\pm,\eta_\pm)+\tilde{Z}_i(\eta_\pm,\eta_\pm),\\
\gamma_i^z(\xi_\pm)&=g_0+C_i(\xi_\pm,\xi_\pm)+\tilde{Z}_i(\xi_\pm,\xi_\pm),\\
\gamma_i^{\tilde{z}}(\xi_\pm)&=g_0+C_i(\xi_\pm,\xi_\pm)+Z_i(\xi_\pm,\xi_\pm);\\
\gamma_i^h(\xi_\pm,\eta_\pm)&=\gamma_i^c(\eta_\pm)+C_i(\xi_\pm,\eta_\pm),\\
\gamma_i^l(\xi_\pm,\eta_\pm)&=\gamma_i^z(\xi_\pm)+Z_i(\xi_\pm,\eta_\pm),\\
\gamma_i^l(\xi_\pm,\eta_\pm)&=\gamma_i^{\tilde{z}}(\xi_\pm)+\tilde{Z}_i(\xi_\pm,\eta_\pm);
\end{aligned} \quad \text{(A15)}$$

and the regions of integration are defined by

$$\begin{aligned}
\int_{c_0}^{A}f(\zeta_+,\zeta_-)&=\int_{-|\xi_+|}^{|\xi_+|}\int_{-|\xi_-|}^{|\xi_-|}d\zeta_+d\zeta_-f(\zeta_+,\zeta_-),\\
\int_{c_0}^{B}f(\zeta_+,\zeta_-)&=\int_{-|\tilde{\xi}_+|}^{|\tilde{\xi}_+|}\int_{-|\tilde{\xi}_-|}^{|\tilde{\xi}_-|}d\zeta_+d\zeta_-f(\zeta_+,\zeta_-),\\
\int_{c_{\mathbf{Q}}}f(\zeta_+,\zeta_-)&=\int_{-|\xi_+|}^{|\xi_+|}\left(\int_{\min\{0,\zeta_-^{(1)}\}}^{\max\{0,\zeta_-^{(1)}\}}+\int_{\min\{-|\xi_-|\mathrm{sign}\zeta_+,\zeta_-^{(2)}\}}^{\max\{-|\xi_-|\mathrm{sign}\zeta_+,\zeta_-^{(2)}\}}\right)\\
&\quad\times\frac{d\zeta_+d\zeta_-}{\cos 2\varphi}\left|\frac{k_+k_-}{k_+^2+k_-^2+2\cos 2\varphi k_+k_-}\right|\\
&\quad\times f(\zeta_+,\zeta_-)+\int_{\min\{0,|\xi_+|\mathrm{sign}\xi_-\}}^{\max\{0,|\xi_+|\mathrm{sign}\xi_-\}}d\zeta_+\\
&\quad\times\left|\frac{\min(\cos 2\varphi k_+,p_-)+p_-}{\cos 2\varphi k_++\sin 2\varphi p_-}\right|f(\zeta_+,\xi_-)\\
&\quad+\int_{\min\{0,|\xi_-|\mathrm{sign}\xi_+\}}^{\max\{0,|\xi_-|\mathrm{sign}\xi_+\}}d\zeta_-\\
&\quad\times\left|\frac{\min(\cos 2\varphi k_-,p_+)+p_+}{\cos 2\varphi k_-+\sin 2\varphi p_+}\right|f(\xi_+,\zeta_-);\\
\int_{z_0}^{A}f(\zeta_+,\zeta_-)&=\int_{-|\eta_+|}^{|\eta_+|}d\zeta_+f(\zeta_+,\eta_-)+\int_{-|\eta_-|}^{|\eta_-|}d\zeta_+f(\eta_+,\zeta_-),\\
\int_{z_0}^{B}f(\zeta_+,\zeta_-)&=\int_{-|\tilde{\eta}_+|}^{|\tilde{\eta}_+|}d\zeta_+f(\zeta_+,\tilde{\eta}_-)+\int_{-|\tilde{\eta}_-|}^{|\tilde{\eta}_-|}d\zeta_+f(\tilde{\eta}_+,\zeta_-),\\
\int_{z_{\mathbf{Q}}}f(\zeta_+,\zeta_-)&=\int_{-|\eta_+|}^{|\eta_+|}\left(\int_{\min\{0,|\eta_-|\mathrm{sign}\zeta_+\}}^{\max\{0,|\eta_-|\mathrm{sign}\zeta_+\}}+\int_{\min\{\zeta_-^{(1)},\zeta_-^{(2)}\}}^{\max\{\zeta_-^{(1)},\zeta_-^{(2)}\}}\right)d\zeta_+d\zeta_-\\
&\quad\times\left|\frac{k_+k_-}{k_+^2+k_-^2+2\cos 2\varphi k_+k_-}\right|f(\zeta_+,\zeta_-);
\end{aligned} \quad \text{(A16)}$$

where

$$\begin{aligned}
k_\pm&=\Lambda\,\mathrm{sgn}(\zeta_\pm)\exp(-|\zeta_\pm|)\\
L(k_\pm)&=\mathrm{sgn}(k_\pm)\ln|\Lambda/k_\pm|\\
\zeta_-^{(1)}&=-L[k_+/\cos 2\varphi]\\
\zeta_-^{(2)}&=-L[k_+/\cos 2\varphi].
\end{aligned}$$

[1] D. J. Scalapino, Phys. Rep. **251**, 1 (1994); J. Low Temp. Phys. **117**, 179 (1999).
[2] N. E. Bickers, D. J. Scalapino, and S. R. White, Phys. Rev. Lett. **62**, 961 (1989).
[3] J. Schmalian, D. Pines, and B. Stojkovic, Phys. Rev. Lett. **80**, 3839 (1998).
[4] A. Chubukov, D. Pines, and B. Stojkovic, J. Phys.: Condens. Matter **8**, 10 017 (1996); A. Chubukov and D. Morr, Phys. Rep. **288**, 355 (1997); A. Abanov and A. Chubukov, Phys. Rev. Lett. **84**, 5608 (2000).
[5] Th. Maier, M. Jarrell, Th. Pruschke, and J. Keller, Phys. Rev. Lett. **85**, 1524 (2000).
[6] S. C. Zhang, Science **275**, 1089 (1997); E. Demler and S. C. Zhang, Nature (London) **396**, 733 (1998).
[7] A. I. Lichtenstein and M. I. Katsnelson, Phys. Rev. B **62**, R9283 (2000).
[8] S. Chakraverty, R. B. Laughlin, D. K. Morr, and C. Nayak, Phys. Rev. B **63**, 094503 (2001).
[9] T. M. Rice and M. Sigrist, J. Phys.: Condens. Matter **7**, L643 (1995).
[10] R. S. Markiewicz, Physica C **217**, 381 (1993); J. Phys. Chem. Solids **58**, 1179 (1997).
[11] A. A. Abrikosov, Physica C **222**, 191 (1994); **233**, 102 (1994).
[12] D. L. Novikov, M. I. Katsnelson, J. Yu, A. V. Postnikov, and A. J. Freeman, Phys. Rev. B **54**, 1313 (1996).
[13] A. I. Liechtenstein, O. Gunnarsson, O. K. Andersen, and R. M. Martin, Phys. Rev. B **54**, 12 505 (1996).
[14] A. Liebsch and A. I. Lichtenstein, Phys. Rev. Lett. **84**, 1591 (2000).
[15] L. V. Keldysh and Yu. V. Kopaev, Fiz. Tverd. Tela (Leningrad) **6**, 2791 (1964).
[16] B. I. Halperin and T. M. Rice, *Solid State Physics* (Academic

Press, New York, 1968), Vo. 21, p. 116.
[17] A. T. Zhelezniak, V. M. Yakovenko, and I. E. Dzyaloshinskii, Phys. Rev. B **55**, 3200 (1997).
[18] D. Zanchi and H. J. Schulz, Europhys. Lett. **44**, 235 (1997); Phys. Rev. B **61**, 13 609 (2000); C. J. Halboth and W. Metzner, *ibid.* **61**, 7364 (2000).
[19] I. E. Dzyaloshinskii, Pis'ma Zh. Eksp. Teor. Fiz. **46** (Suppl.), 110 (1987); Zh. Eksp. Teor. Fiz. **93**, 1487 (1987) [Sov. Phys. JETP **66**, 848 (1987)].
[20] Yu. A. Bychkov, L. P. Gor'kov, and I. E. Dzyaloshinskii, Zh. Eksp. Teor. Fiz. **50**, 738 (1966) [Sov. Phys. JETP **23**, 489 (1966)].
[21] I. E. Dzyaloshinskii and A. I. Larkin, Zh. Eksp. Teor. Fiz. **61**, 791 (1971) [Sov. Phys. JETP **34**, 422 (1972)].
[22] I. E. Dzyaloshinskii and E. I. Kaz, Zh. Eksp. Teor. Fiz. **62**, 1104 (1972) [Sov. Phys. JETP **35**, 584 (1972)].
[23] I. E. Dzyaloshinskii, J. Phys. I **6**, 119 (1996).
[24] T. Tohyama and S. Maekawa, Supercond. Sci. Technol. **13**, R17 (2000).
[25] I. E. Dzyaloshinskii and V. M. Yakovenko, Zh. Eksp. Teor. Fiz. **94**, 344 (1988) [Sov. Phys. JETP **67**, 844 (1988)].
[26] C. Honerkamp, M. Salmhofer, N. Furukawa, and T. M. Rice, Phys. Rev. B **63**, 035109 (2001).
[27] R. Shankar, Rev. Mod. Phys. **66**, 129 (1994).
[28] J. V. Alvarez, J. Gonzalez, F. Guinea, and M. A. H. Vozmediano, J. Phys. Soc. Jpn. **67**, 1868 (1998).
[29] M. Fleck, A. Oles, and L. Hedin, Phys. Rev. B **56**, 3159 (1997).
[30] R. Hlubina, S. Sorella, and F. Guinea, Phys. Rev. Lett. **78**, 1343 (1997).
[31] P. Lederer, G. Montambaux, and D. Poilblanc, J. Phys. (Paris) **48**, 1613 (1987).
[32] N. Furukawa, T. M. Rice, and M. Salmhofer, Phys. Rev. Lett. **81**, 3195 (1998).
[33] J. Solyom, Adv. Phys. **28**, 201 (1979).
[34] V. Janis, in *Proceedings of the International Workshop on Electron Correlations and Material Properties*, edited by A. Gonis and N. Kioussis (Plenum Press, New York, 1999).
[35] V. V. Sudakov, Dokl. Akad. Nauk SSSR **111**, 338 (1956) [Sov. Phys. Dokl. **1**, 662 (1957)].
[36] C. M. Varma, P. B. Littlewood, S. Schmitt-Rink, E. Abrahams, and A. E. Ruckenstein, Phys. Rev. Lett. **63**, 1996 (1989); **64**, 497 (1990).
[37] D. Menashe and B. Laikhtman, Phys. Rev. B **59**, 13 592 (1999).
[38] T. Moriya, *Spin Fluctuations in Itinerant Electron Magnetism* (Springer, Berlin, 1985).
[39] V. Yu. Irkhin, M. I. Katsnelson, and A. V. Trefilov, J. Magn. Magn. Mater. **117**, 210 (1992); J. Phys.: Condens. Matter **5**, 8763 (1993).
[40] M. I. Katsnelson, G. V. Peschanskikh, and A. V. Trefilov, Fiz. Tverd. Tela (Leningrad) **32**, 570 (1990); M. I. Katsnelson, I. I. Naumov, and A. V. Trefilov, Phase Transitions **49**, 143 (1994).